

Steps To Demarcate the Effects of Chromophore Aggregation and Planarization in Poly(phenyleneethynylene)s. 2. The Photophysics of 1,4-Diethynyl-2-fluorobenzene in Solution and in Crystals

Marcia Levitus, Gerardo Zepeda, Hung Dang, Carlos Godinez, Tinh-Alfredo V. Khuong, Kelli Schmieder, and Miguel A. Garcia-Garibay*

Department of Chemistry and Biochemistry, The University of California,
Los Angeles, California 90095-1569

mgg@chem.ucla.edu

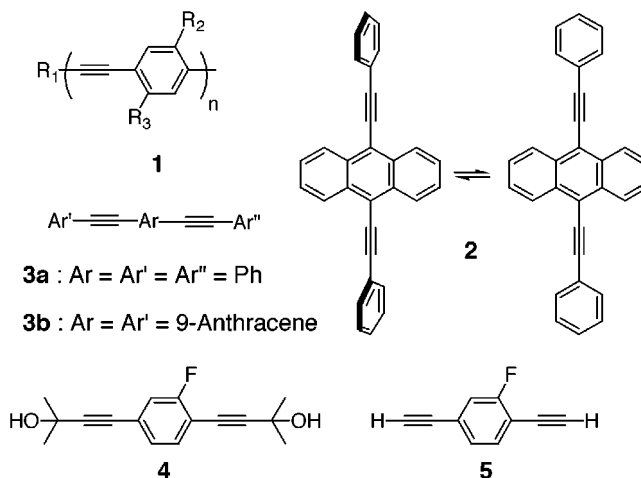
Received February 22, 2001

Crystals of 1,4-bis(2-hydroxy-2-methyl-3-butynyl)-2-fluorobenzene **4** have a rich packing structure with four distinct molecules in the unit cell. A complex hydrogen bonding network results in the formation of cofacial trimers, cofacial dimers, and monomers within the same unit cell. Given a remarkable opportunity to investigate the effect of aggregation on the photophysics of 1,4-diethynylbenzenes, we analyzed the absorption, diffuse reflectance, and emission spectra of compound **4** in solutions and in crystals. Diffuse reflectance and fluorescence excitation revealed a red-shifted absorption that is absent in dilute solution but becomes observable at high concentrations and low temperatures. The fluorescence emission in the solid state is dual with components assigned to monomers and aggregates. The excitation and emission assigned to the monomer are nearly identical in crystals and dilute solutions. The absorption and emission bands assigned to aggregates are broad and red-shifted by 60–80 nm. As expected for a sample with absorbers and emitters with different energies and incomplete equilibration, efficient monomer-to-aggregate energy transfer was observed by a proper selection of excitation wavelengths. The fluorescence quantum yield of **4** in solution is relatively low ($\Phi_F = 0.15$) and the singlet lifetime short ($\tau_F = 3.8$ ns). A lower limit for the triplet yield of $\Phi_T = 0.64$ was determined indirectly in solution by 1O_2 sensitization, and a relatively strong and long-lived phosphorescence was observed in low-temperature glasses and in crystals at 77 K.

Introduction

Several poly(phenyleneethynylene)s (**1**)^{1,2} and other aryethynyl fluorophores (e.g., **2–5**, Scheme 1),³ have become very attractive for a wide variety of photonics and sensing applications due to their electron-transport abilities and intense fluorescence emission. Among their many interesting properties, red shifts in the absorption and emission spectra are frequently observed upon concentration and thin film formation⁴ and by addition of nonsolvents.⁵ Although these spectral changes and the observation of self-quenching have been primarily explained in terms of aggregation effects, possible contributions from coplanarization and twisting of the aryl groups

Scheme 1



(1) (a) Bunz, U. H. F. *Chem. Rev.* **2000**, *100*, 1605–1644. (b) Levitsky, I. A.; Kim, J.; Swager, T. M. *J. Am. Chem. Soc.* **1999**, *121*, 1466–1472. (c) Sato, T.; Jiang, D.-L.; Aida, T. *J. Am. Chem. Soc.* **1999**, *121*, 10658–10659. (d) Samori, P.; Francke, V.; Müllen, K.; Rabe, J. P. *Chem. Eur. J.* **1999**, *5*, 2312–2317.

(2) (a) McQuade, D. T.; Pullen, A. E.; Swager, T. M. *Chem. Rev.* **2000**, *100*, 2537–2574, and references therein.

(3) (a) Hanhela, P. J.; B. D. P. *Aust. J. Chem.* **1984**, *37*, 553. (b) Gisser, D. J.; Johnson, B. S.; Ediger, M. D.; Von Meerwall, E. D. *Macromolecules* **1993**, *26*, 512. (c) Lindasy, J. S.; Prahapan, S.; Johnson, T. E.; Wagner, R. W. *Tetrahedron* **1994**, *50*, 8941–8968.

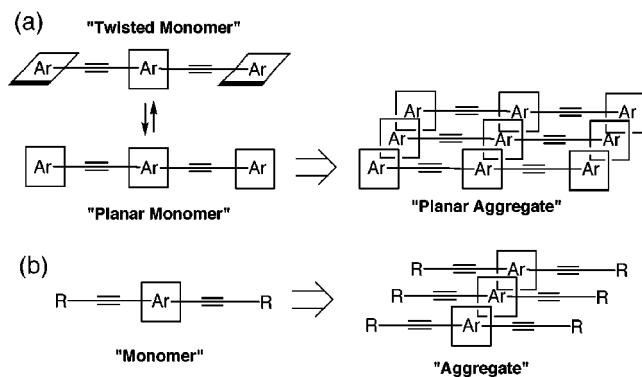
(4) (a) McQuade, D. T.; Kim, J.; Swager, T. M. *J. Am. Chem. Soc.*, **2000**, *122*, 5885–5886. (b) Walters, K. A.; Ley, K. D.; Schanze, K. S. *Langmuir* **1999**, *15*, 5676–5680. (c) Weder, C.; Wrighton, M. S. *Macromolecules* **1996**, *29*, 5157–5165.

(5) (a) Miteva, T.; Palmer, L.; Kloppenburg, L.; Neher, D.; Bunz, U. H. F. *Macromolecules* **2000**, *33*, 652–654. (b) Halkyard, C. E.; Rampey, M. E.; Kloppenburg, L.; Studer-Martinez, S. L.; Bunz, U. H. F. *Macromolecules* **1998**, *31*, 8655.

have been recently suggested by Bunz et al. (Scheme 2).^{5,6} While it is reasonable that both planarization and aggregation may have an effect on ground and excited state properties of aryethynyl-containing compounds, the separation of these effects has been difficult to factorize and remains somewhat controversial.^{4a} Ambiguities may arise because spectroscopic manifestations of chro-

(6) Planarization effects on the electronic properties of conducting polymers had been previously reported by Wudl and co-workers: Rughooopath, S. D. D. V.; Hotta, S.; Heeger, A. J.; Wudl, F. *J. Polym. Sci. B* **1987**, *25*, 1071.

Scheme 2



mophore aggregation are known to involve cofacial interactions between molecules that are in *planar conformations* (Scheme 2a).^{2,7,8} To our knowledge, there are no aggregates formed by twisted arylethyne that can be detected by absorption or fluorescence changes, and it is difficult to prevent the aggregation of planar aromatic compounds. To prepare highly luminescent solid state materials, synthetic strategies based on the use of bulky substituents that minimize aggregation have encountered remarkable success.⁹ However, the results obtained in those cases have not addressed the possible contributions from planarization effects.

In a recent study with 9,10-bis(phenylethynyl) anthracene **2** (Scheme 1), we noticed that conditions affecting the planarization and conformational dynamics of the three aryl rings led to significant changes in the absorption spectrum.¹⁰ A recently reported study with 1,4-bis(phenylethynyl)benzene,¹¹ and work in progress on other compounds,¹² suggests that the conformation-dependent photophysics of compound **2** may be a general property of alkyne-conjugated aromatic chromophores. While preparing a series of 1,4-diethynyl derivatives, we came across samples of 1,4-diethynyl-2-fluorobenzene **5** and its acetone-protected precursor **4** (Scheme 1). Recognizing that 1,4-diethynylbenzenes would be the simplest arylethynyl chromophore with photophysical properties independent of phenyl group rotation, we decided to investigate their properties in solution and in crystals.¹³ As illustrated in Scheme 2b, we reasoned that compounds **4** and **5** may illustrate the effects of aggregation without complications from planarization of aryl groups linked to the triple bonds. We report here the results obtained

with these compounds. While only limited measurements were carried out with **5**, due to its rapid decomposition, detailed results with compound **4** as a function of concentration and in the solid state revealed several differences between monomer and aggregate emission. The aggregate emission was characterized by broad and red-shifted spectra and by longer fluorescence lifetimes. The results obtained in the solid state, including photophysical measurements and solid state ¹³C NMR, were analyzed in terms of the unusually rich and complex X-ray structure of compound **4**.

Experimental Section

General. Reagents and solvents of the highest commercial purity were purchased from Fisher or Aldrich and were used as received. IR spectra were acquired on a Perkin-Elmer Paragon 1000 FT-IR instrument. ¹H(¹³C) NMR spectra were obtained on Bruker ARX NMR spectrometer operating at 400 and 500 MHz for ¹H and at 100 or 125 MHz for ¹³C in CDCl₃ with TMS as internal standard. Gas chromatographic analyses (GC) were conducted on a Hewlett-Packard 5890 Series II capillary instrument equipped with a flame ionization detector (FID) and a Hewlett-Packard 3396 Series II integrator. Melting points were determined with a Fisher-Johns melting point apparatus.

1,4-Bis(2-hydroxy-2-methyl-3-butynyl)-2-fluorobenzene (4). Compound **4** was prepared using a modification of the method reported in the literature.¹⁴ 1,4-Dibromo-2-fluorobenzene (1.15 g, 4.5 mmol), (PPh₃)₂PdCl₂ (0.31 g, 0.44 mmol), and 2-methyl-3-butyn-2-ol (0.93 g, 11.0 mmol) were dissolved in 10 mL of piperidine in a three-neck round-bottom flask equipped with a condenser and kept under an Ar atmosphere. The mixture was refluxed for 4 h, and workup was carried out by addition of 50 mL of ether before washing the organic layer successively with 15 mL of water, dilute HCl, and brine. The organic layer was dried over anhydrous MgSO₄ and evaporated to near dryness at low temperature avoiding high vacuum. The product was purified by column chromatography (hexanes:ethyl acetate 4:1 v/v) to afford 0.67 g, 56% yield, of a pale yellow crystalline solid: mp 134.5–135.0 °C; ¹H NMR (500 MHz, CDCl₃) δ 1.61 (s, 6H, -CH₃), 1.63 (s, 6H, CH₃), 2.32 (broad, 2H, OH), 7.10 (m, 1H, Ar), 7.12 (m, 1H, Ar), 7.31 (m, 1H, Ar); ¹³C NMR (125 MHz, CDCl₃) δ 31.26, 31.28, 65.44, 65.62 (d, *J*_{CF} = 56.5 Hz), 75.23, 80.67 (d, *J*_{CF} = 12.5 Hz), 96.28, 100.51, 111.49 (d, *J*_{CF} = 63.5 Hz), 118.41 (d, *J*_{CF} = 90.5 Hz), 124.39 (d, *J*_{CF} = 37.5 Hz), 127.24 (d, *J*_{CF} = 14 Hz), 133.18 (d, *J*_{CF} = 7.5 Hz), 162.05 (d, *J*_{CF} = 1001 Hz); IR (KBr) cm⁻¹ = 3365.6, 3087.5, 3087.5, 2982.3, 1615.6, 1363.6, 1124.0; MS (70 eV) *m/z* (rel intensity) = 260 (65, M⁺), 245 (100), 227, (40), 187 (20). Details of the crystal structure of **4** are included in the Supporting Information section.

1,4-Diethynyl-2-fluorobenzene (5). Compound **4** (0.2 mg, 0.768 mmol), potassium hydroxide (0.3 g, 5.36 mmol), tetrabutylammonium iodide (0.5 g, 1.35 mmol), and 10 mL of benzene were added to a round-bottom flask equipped with a condenser and heated to 50 °C under an Ar atmosphere. The yellow-orange suspension was stirred for 12 h and monitored by TLC. Workup was carried out by adding 50 mL of diethyl ether before washing the organic layer successively with 15 mL of water, dilute hydrochloric acid, and brine. The organic layer was dried over anhydrous MgSO₄ and evaporated to near dryness at low temperature avoiding high vacuum. The product was purified by column chromatography using pentane as the eluant to yield 80 mg (56% isolated yield) of the pure product as a pale yellow solid which exhibited a high vapor pressure as well as high thermal and light sensitivity: ¹H NMR (400 MHz, CDCl₃) δ 3.21 (s, 1H), 3.39 (s, 1H), 7.19–7.23 (m, 2H), 7.40–7.44 (m, 1H); ¹³C NMR (100 MHz, CDCl₃) δ 76.5, 80.1, 81.8 (d, *J*_{CF} = 12.4 Hz), 84.2 (d, *J*_{CF} = 13.6 Hz), 111.5 (d, *J*_{CF} = 63.2 Hz), 119.1 (d, *J*_{CF} = 90.4 Hz), 124.4 (d,

(7) Li, H.; Powell, D. R.; Hayashi, R. K.; West, R. *Macromolecules* **1998**, *31*, 52–58.

(8) (a) Bredas, J. L.; Cornil, J.; Bejonne, D.; dos Santos, D. A.; Shuai, Z. *Acc. Chem. Res.* **1999**, *32*, 267. (b) Cornil, J.; Dos Santos, D. A.; Crispin, X.; Silbey, R.; Bredas, J. L. *J. Am. Chem. Soc.* **1998**, *120*, 1289–1299. (c) Bejonne, D.; Cornil, J.; Silbey, R.; Millié, P.; Brédas, J. L. *J. Chem. Phys.* **2000**, *112*, 4749–4758.

(9) (a) Williams, V. E.; Swager, T. M. *Macromolecules* **2000**, *33*, 4069–4073. (b) Yang, J.-S.; Swager, T. M. *J. Am. Chem. Soc.* **1998**, *120*, 11864–11873.

(10) Levitus, M.; Garcia-Garibay, M. A. *J. Phys. Chem. A* **2000**, *104*, 8632–8637.

(11) Levitus, M.; Schmieder, J.; Ricks, H.; Bunz, U. H. F.; Garcia-Garibay, M. A. Manuscript in preparation.

(12) Levitus, M.; Schmieder, K.; Garcia-Garibay, M. A. Manuscript in preparation.

(13) We were surprised to find out that the photophysics of 1,4-diethynylbenzene have been only scarcely investigated, see: (a) Laposa, J. D. *J. Lumin.* **1979**, *20*, 67–72. (b) Sazhnikov, V. A.; Razumov, V. F.; Alfimov, M. V. *Opt. Spektrosk.* **1978**, *44*, 196–198. (c) Razumov, V. F.; Sazhnikov, V. A.; Alfimov, M. V.; Kotlyarevskii, I. L.; Bardamova, M. I.; Vasilevskii, S. F. *Izv. Akad. Nauk SSSR, Ser. Khim.* **1979**, *2*, 358–362.

(14) Pugh, C.; Percec, V. *Polym. Bull.* **1990**, *23*, 177–184.

$J_{CF} = 37.2$ Hz), 127.8 (d, $J_{CF} = 14.4$ Hz), 133.8 (d, $J_{CF} = 7.6$ Hz), 162.7 (d, $J_{CF} = 1006.4$ Hz).

UV-Vis and Fluorescence. Absorption spectra were recorded in a Hewlett-Packard 8453 UV-vis or a Shimadzu 3101-PC UV-Vis-NIR spectrometer. A diffuse reflectance accessory was attached to the Shimadzu spectrometer for diffuse reflectance measurements, which were carried out with properly characterized crystalline powdered samples using BaSO_4 as a reference. Fluorescence spectra were recorded in a Spex-Fluorolog II spectrometer and were corrected for nonlinear detector response. Compounds **4** and **5** were purified by column chromatography and by recrystallization until their fluorescence emission in solution was independent of the excitation wavelength. Fluorescence decays were measured with a time-correlated single photon counting fluorimeter (Edinburgh Instruments, model FL900CDT) equipped with a pulsed H_2 discharge lamp operating at 0.4 bar (fwhm ~ 0.7 ns). Signal intensities were attenuated to detect photons at a rate of 1% of the excitation source repetition rate operating at 40 kHz. The instrumental response recorded with scattered light from a LUDOX suspension was used to deconvolute the short-lived fluorescence signals from the excitation pulse intensity profile. Measurements with solid samples and with amorphous glasses at 77 K were carried out by exciting the sample with vertically polarized light and setting the emission polarizer at the magic angle to eliminate polarization effects.

X-ray Structure Determination. Crystals of compound **4** ($\text{C}_{16}\text{H}_{17}\text{FO}_2$) were grown by slow evaporation from mixtures of benzene and hexanes. A pale yellow needle with approximate dimensions of 0.6 mm \times 0.2 mm \times 0.1 mm was used for X-ray crystallographic analysis. The X-ray intensity data were measured at 298 K on a Bruker SMART 1000 CCD-based X-ray diffractometer system equipped with a Mo-target X-ray tube ($\lambda = 0.71073$ Å) operated at 2250 W power. The detector was placed at a distance of 4.986 cm from the crystal. A total of 1321 frames were collected with a scan width of 0.3° in ω , with an exposure time of 30 s/frame. The frames were integrated with the Bruker SAINT software package using a narrow-frame integration algorithm. The integration of the data using a triclinic unit cell yielded a total of 14183 reflections to a maximum θ angle of 28.31° , of which 9779 were independent and 3440 (35%) were greater than $2\sigma(I)$. The final unit cell contents of $a = 6.0599(10)$ Å, $b = 17.450(3)$ Å, $c = 21.186(3)$ Å, $\alpha = 101.422(3)^\circ$, $\beta = 95.053(3)^\circ$, $\gamma = 92.618(3)^\circ$, and volume = $2182.7(6)$ Å³ are based upon the refinement of the xyz centroids of 870 reflections above $20\sigma(I)$. Analysis of the data showed negligible decay during data collection. The structure was refined on the basis of the space group $P\bar{1}$ with $Z = 6$, using the Bruker SHELXTL (Version 5.3) software package. The final anisotropic full-matrix least-squares refinement on F^2 converged at $R1 = 5.78\%$ [$I > 2\sigma(I)$], $wR2 = 16.21\%$, and a goodness of fit of 0.818. The largest peak on the final difference map was 0.378 e/Å³. The calculated density for $\text{C}_{16}\text{H}_{17}\text{FO}_2$ is 1.188 Mg/m³ and $F(000)$ is 828e.

Solid State ¹³C CPMAS NMR. Solid state ¹³C NMR spectra were acquired at ambient temperature on a Bruker Avance 300 NMR instrument operating at 75 MHz by cross-polarization and magic angle spinning (CPMAS). Powdered samples packed in 4 mm i.d. rotors were spun at 10 kHz. Hydrogens were polarized with 4 μs 90° pulses and cross-polarization was carried out with contact times of 4 ms. Relaxation delays were set to 5 s. Quaternary signals were assigned by using a 50 μs dipolar-dephasing delay immediately after cross-polarization.¹⁵

Results and Discussion

Absorption and Emission Spectra in Dilute Solution. We were able to show that the UV-vis and fluorescence spectra of **4** and **5** in dilute cyclohexane solutions at ambient temperature are essentially identical to each other and in agreement with published spectra

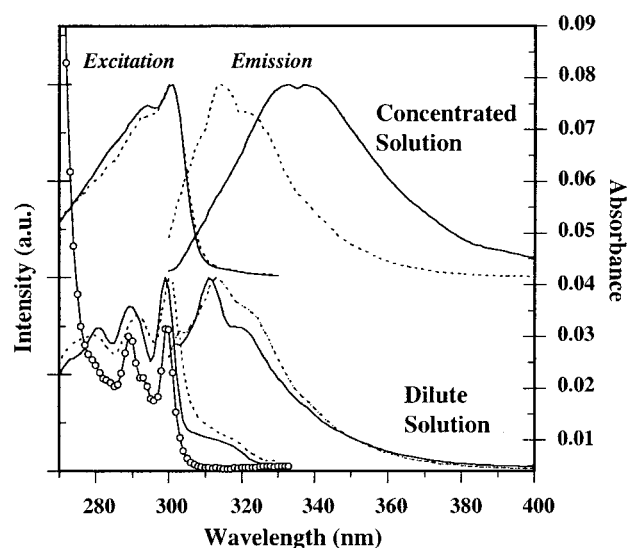


Figure 1. Fluorescence excitation and emission of 1,4-diethynyl-2-fluorobenzene **4** in dilute and concentrated solutions in methylcyclohexane at 298 K (dotted lines) and at 77 K (filled lines). The absorption spectrum is marked with circles and goes with the scale on the right.

of the parent 1,4-diethynylbenzene¹³ (Figure 1). In agreement with the well-documented chemical instability of 1,4-diethynylbenzene,¹⁶ the terminal alkyne **5** was found to decompose within a few hours at ambient temperature, or after a few days when stored at -20°C . The absorption spectrum of the protected compound **4** in the UV region consists of three overlapping bands centered at 270 ($\epsilon = 4 \times 10^4$ M⁻¹ cm⁻¹), 290, and 300 nm ($\epsilon = 1.2 \times 10^4$ M⁻¹ cm⁻¹). The emission spectrum in methylcyclohexane solution at ambient temperature extends from 300 to 400 nm with a λ_{max} at ca. 312 nm. The emission quantum yields determined for **4** and **5** were the same, with a value of $\Phi_F = 0.15(\pm 0.02)$. Fluorescence decays in cyclohexane solutions were determined by time-correlated single photon counting and were fit to single exponentials which gave lifetimes of 2.0 (± 0.1) ns and 3.8 (± 0.1) ns for compounds **4** and **5**, respectively. Given its higher stability and interesting solid state structure (see below), most detailed measurements were carried out with compound **4**.

Absorption and Emission Spectra of Compound 4 in Concentrated Solution at 298 and 77 K. In search of experimental evidence for intermolecular aggregation in the 1,4-diethynyl-2-fluorobenzene chromophore, we carried out a series of measurements as a function of concentration. We reasoned that compound **4** may take advantage of weak hydrogen bonding in nonpolar solvents to form spectroscopically observable cofacial dimers (Scheme 3).

As illustrated by the spectra shown with dotted lines in Figure 1, measurements in methylcyclohexane at 298 K resulted in relatively small changes on either excitation or emission signals with samples at concentrations ranging from 7×10^{-2} to 1.7×10^{-6} M (Table 1). Although the fluorescence lifetimes of concentrated samples at 298 K were slightly longer ($\tau = 2.2 \pm 0.1$ ns) than those obtained in dilute solutions ($\tau = 2.0 \pm 0.1$ ns), no evidence

(15) Opella, S. J.; Frey, M. H. *J. Am. Chem. Soc.* **1979**, *101*, 5854.

(16) (a) Gottfried, C.; Walter, R. *Chem. Ber.* **1975**, *108*, 528–537. (b) Petrus, A. A. *Khim. Vis. Energ.* **1974**, *8*, 280–281; *Chem. Abstr.* **1974**, *81*, 78329.

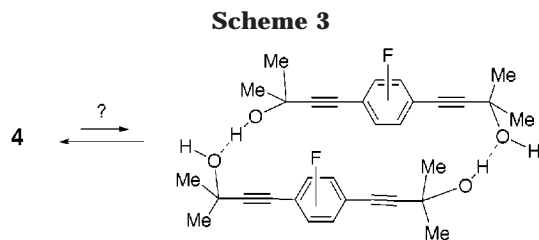


Table 1. Photophysical Properties of Compound 4 under Various Experimental Conditions^a

solvent	concn [M]	temp (K)	λ_{\max} (nm)	τ_F (ns) ^b
MCH	1.7×10^6	300	310	2.0
MCH	7×10^{-2}	300	310	2.2
MCH	1.7×10^6	77	310	3.0, 0.4 ^c
MCH	7×10^{-2}	77	332	8.5, 2.4 ^c
crystal		300	330	<i>d</i>
crystal		300	430	<i>d</i>

^a All samples were thoroughly deoxygenated before measurements. ^b Estimated errors in lifetimes are within 0.1 ns. ^c Decays were satisfactorily fit to double exponential functions. ^d Decays were too complex to fit to one or two exponentials.

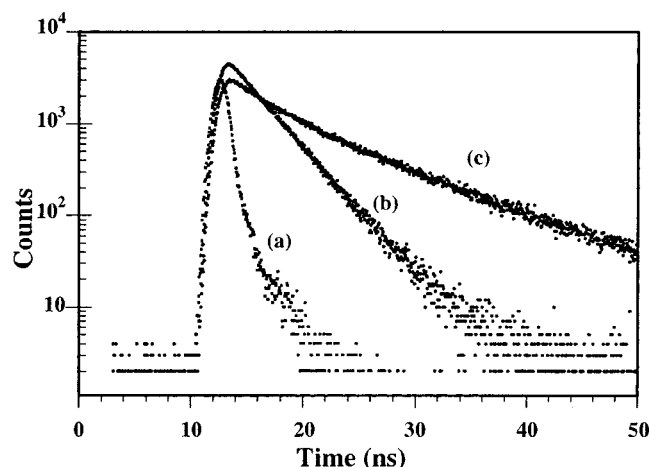


Figure 2. Lamp profile (a) and double exponential fluorescence decay (b) of compound **4** in dilute ($\tau_1 = 3.0$ and $\tau_2 = 0.4$ ns) and (c) concentrated ($\tau_1 = 8.5$ and $\tau_2 = 2.4$ ns) methylcyclohexane glasses at 77 K.

for aggregation was obtained from ¹H NMR spectra recorded in CDCl₃ with samples prepared over a 100-fold concentration range. The combined effects of high sample concentration and low temperatures gave rise to observable aggregation effects on the fluorescence spectra (Figure 1, top spectra). While fluorescence measurements with dilute samples at 77 K in MCH (methylcyclohexane) showed only small changes as compared to those at 298 K, measurements carried out with concentrated samples at the same low temperature resulted in severe broadening and a 30–40 nm red shift in the λ_{\max} of the emission spectrum. We interpret these results as an indication of a very weak cofacial association that gives rise to weakly interacting aggregates. Although relatively small changes were observed in the excitation spectra, lifetime measurements for the aggregated and monomeric species at 77 K were significantly different (Table 1). Decays at 77 K were fit to double-exponential functions with lifetimes of 3.0 and 0.4 ns for the monomer and 8.5 and 2.4 ns for the aggregate (Figure 2). It may be noted that a small increase in the lifetime of the monomer at low temperature suggests that contributions of thermal decay at ambient temperature should be relatively small.

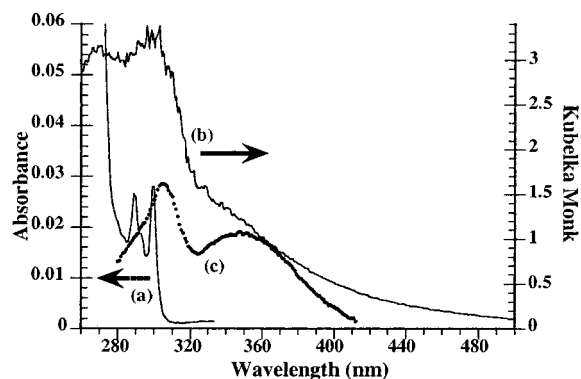


Figure 3. Electronic absorption spectra of 1,4-diethynyl-2-fluorobenzene **4** obtained under different experimental conditions: (a) UV-vis absorption spectrum in hexane solution, (b) diffuse reflectance spectrum in the crystalline solid state (given in Kubelka-Monk units), and (c) fluorescence excitation in the solid state (in arbitrary units).

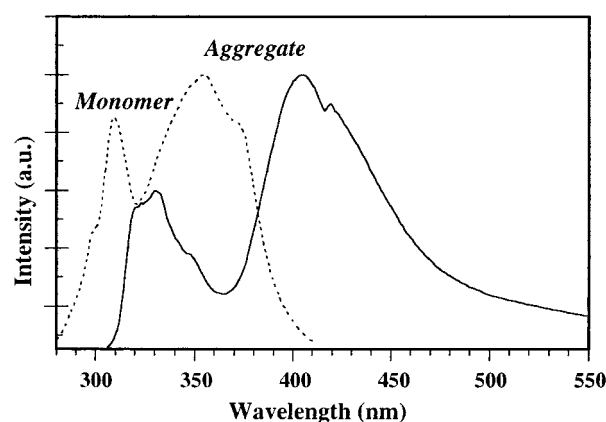


Figure 4. Fluorescence excitation (dotted line) and emission (filled line) of compound **4** in a polycrystalline sample. Bands assigned to monomer and aggregate are labeled on the top.

Diffuse Reflectance and Emission in Crystals of 4. Since formation of spectroscopically detectable aggregates in the solid state is relatively common, we carried out diffuse reflectance and fluorescence measurements with crystals of compound **4**. As illustrated in Figure 3, we found with satisfaction that the diffuse reflectance spectra from fine-powder samples revealed a broad band between 320 and 400 nm that is significantly red-shifted with respect to the lowest energy absorption band that we had measured in dilute solutions.¹⁷ The formation of a new chromophore in the solid state was also evident from the fluorescence excitation and emission measurements shown in Figure 4. Two excitation and emission band systems were clearly distinguished by measurements carried out by front-face illumination and detection. The position of one of the excitation and emission band systems in the solid state resembles the position of the excitation and emission spectra in dilute solution, suggesting a monomeric species. The second band system is more intense and red-shifted by approximately 60–80 nm (Figure 4), and it has an excitation spectrum that is in excellent agreement with the red-shifted absorption determined by diffuse reflectance methods.

(17) Selected spectra, X-ray diagrams, and X-ray tables can be found in the Supporting Information.

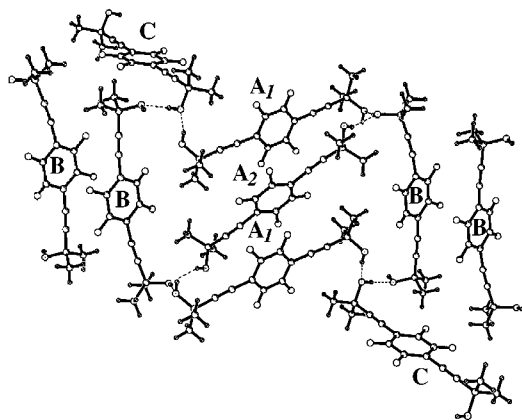


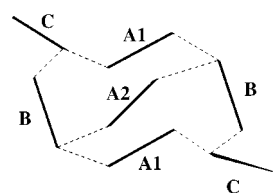
Figure 5. Packing motif of molecules of 1,4-bis(2-hydroxy-2-methyl-3-butynyl)-2-fluorobenzene **4** illustrating its association in offset trimers (A), dimers (B), and monomers (C). Fluorine atoms are evenly disordered through the four aromatic groups. See text for more detailed description.

X-ray Crystal Structure. The packing structure of **4** is remarkably complex and structurally rich and accounts satisfactorily for the photophysical observations illustrated in Figures 3 and 4. Slow evaporation of hexanes–benzene solutions of **4** yielded triclinic crystals with space group $P\bar{1}$ having the unusual number of six molecules per unit cell.¹⁷ Even more remarkable is the fact that there are four structurally different molecules in the crystal. Two molecules sit in general crystallographic positions and two centrosymmetric molecules sit at crystallographic inversion centers. This arrangement gives a total of three independent molecules per unit cell (i.e., two full molecules plus two halves). From the four structurally different molecules in the crystal, two are essentially planar and the other two have alkyne groups bent away from the plane of their phenyl rings. The fluorine substituents are disordered through the four positions of the phenyl rings, creating a space-disordered packing structure. The structure was refined by a full-matrix least-squares procedure on F^2 , giving $R_1 = 0.0578$ for $I > 2\sigma I$ and $wR_2 = 0.1621$ for all the diffraction data.

The packing structure of **4** is shown in Figure 5 from a view that illustrates layers of molecules on the (100) plane. Molecules labeled A, B, and C have their long molecular axes roughly parallel to the (100) plane and the planes of their phenyl groups tilted from the normal. At the center of the cluster shown is a sandwich-like trimeric aggregate with molecules labeled A_1 – A_2 – A_1 (Figure 5). The long molecular axis and the plane of molecule A_2 are offset from the axes, and the planes of the two molecules A_1 on the outside of the trimer. Although the center-to-center distance between the middle molecule and either of the two outside molecules is 4.58 Å, close contacts between alkyne and aryl carbons are as small as 3.087 Å. The central trimer in Figure 5 is flanked on the sides by two dimers of bent molecules having cofacial phenyl rings with intermolecular contacts as short as 3.51 Å and aromatic center-to-center distances of 4.38 Å. These are labeled B in Figure 5.

Edge-on views illustrating the bending, cofacial interaction, and relative displacement in molecules A and B are shown in Figure 6. Also shown is an edge-on view of a molecule C, which has no close cofacial contacts. Molecules A, B, and C translate down the a -axis in a staircase-like arrangement with intermolecular distances

Scheme 4



of 6.06 Å (not shown). It is also worth noting that all the hydroxyl groups in the structure of **4** are involved in a complex three-dimensional H-bonding network that is schematically illustrated in Scheme 4. The observed H-bonding pattern can be described in terms of a heptameric cyclic array that encloses molecule A_2 . The enclosure is formed by molecules C – A_1 – B – C – A_1 – B , and molecules A_2 are held inside the “box” by hydrogen bonding to the hydroxyl oxygen of molecules B located at opposite corners of the box. As indicated in Figure 5 and Scheme 4, molecules C experience simultaneous H-bond to B and A_1 of adjacent “boxes” while molecules B hydrogen bond to A_1 , A_2 , and C.

Solid State ^{13}C CPMAS NMR. The solid state ^{13}C NMR of compound **4** was obtained with cross-polarization and magic angle spinning (CPMAS) to document the strain and intermolecular interactions that are present in the crystal. The isotropic ^{13}C NMR solution spectrum of **4** consists of 14 signals spanning from 30 to 162 ppm, with ^{13}C – ^{19}F scalar coupling constants for aromatic and alkyne carbons ranging between 7.5 and 1001 Hz. Although three nonequivalent molecules in the unit cell of **4** may be expected to give as many as 42 distinguishable signals, only 12 groups of broad or partially resolved signals were observable in the solid state spectrum (Figure 7). An easily distinguishable ^{13}C – ^{19}F scalar coupling in the solid state was observed only for the ipso C–F carbon at 162 ppm. Alkyne signals near 78 and 90 ppm and aromatic signals between 110 and 165 ppm are heterogeneously broadened by the relative large number of nonequivalent nuclei from crystallographically different molecules and by residual scalar coupling (see inset in Figure 7). It is interesting that the dispersion in chemical shifts falls within ca. 5–6 ppm (~450 Hz) for most carbon signals. This is a relatively narrow range given the presence of molecules with severe distortions from planarity and molecules with a variety of hydrogen bonding and aromatic stacking interactions.

Solid State Photophysics. It is well-known that aggregation may cause large spectral shifts and band shape changes. Several investigators have correlated X-ray structural data with photophysical properties in the crystalline solid state to document the nature of interchromophore interactions.¹⁸ Qualitatively, molecular excitation theory predicts that spectral shifts will depend on the electrostatic interaction between the transition dipole moments of neighboring molecules.^{19,20} These interactions

(18) (a) Lewis, F. D.; Yang, J.-S.; Stern, C. L. *J. Am. Chem. Soc.* **1996**, *118*, 2772–2773. (b) Lewis, F. D.; Yang, J.-S. *J. Phys. Chem. B* **1997**, *101*, 1775–1781. (c) Singh, A. K.; Krishna, T. S. R. *J. Phys. Chem. A* **1997**, *101*, 3066–3069. (d) Brinkman, M.; Gadret, G.; Muccini, M.; Taliani, C.; Masciochi, N.; Sironi, A. *J. Am. Chem. Soc.* **2000**, *122*, 5147–5157.

(19) (a) McRae, E. G.; Kasha, M. *J. Chem. Phys.* **1958**, *28*, 721–722. (b) Hochstrasser, R. M.; Kasha, M. *Photochem. Photobiol.* **1964**, *3*, 317–331.

(20) (a) Siddiqui, S.; Spano, F. C. *Chem. Phys. Lett.* **1999**, *308*, 99–105. (b) Burshtein, K. Y.; Bagatu'yants, A. A.; Alfimov, M. V. *Chem. Phys. Lett.* **1995**, *239*, 195–200.

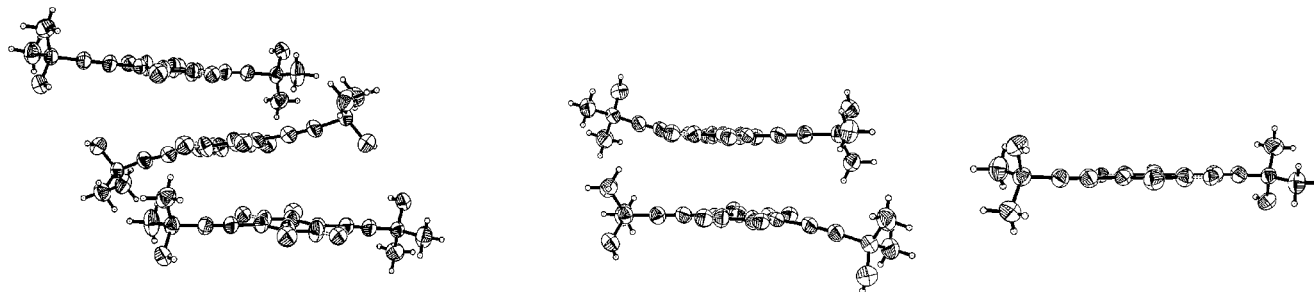


Figure 6. Ortep diagrams of molecules **4** illustrating their interaction in trimeric (left), dimeric (center), and monomeric arrangements (right). All molecules translate along similar staircase-like chains.

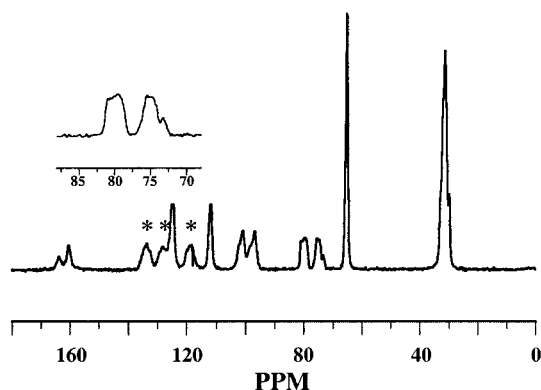


Figure 7. ^{13}C CPMAS NMR spectrum of compound **4**. Protonated aromatic signals identified by dipolar decoupling are indicated with an asterisk. Signals corresponding to alkyne carbons attached to the phenyl group shown in expansion.

are strongly dependent on aggregate size and geometry, leading to blue-shifts (H-aggregates), red-shifts (J-aggregates), and/or spectral broadening, depending on which of the aggregate transitions are symmetry allowed. It has been shown that close cofacial interactions are among the strongest.^{7,21} In the case of compound **4**, discrete aggregates and monomers were found by single-crystal X-ray diffraction analysis. In analogy with other examples reported in the literature, the red-shifted absorption (300–380 nm) and emission (360–550 nm) is probably determined by the strongly interacting dimeric (B–B) and trimeric aggregates (A1–A2–A1) and the blue-shifted bands by the weakly interacting monomeric species (C).¹⁸ Several studies suggest that red shifts require coplanar molecules at distances of 4 Å or less, which must be displaced from a perfect parallel alignment.^{7,19,20} An additional aspect to consider in the case of compound **4** comes from the distortion of molecules constituting the dimer (B) and the central molecule in the trimer (A2) and from the positional disorder of the fluorine atom.²² As shown in Figure 8, results from semiempirical spectroscopic calculations suggest that these factors may cause only small changes to the electronic spectra of isolated molecules. Single-point ground state energies were calculated with the AM1 method using the X-ray coordinates of molecules A, B, and C as defined in Figure 3, and their electronic transition energies were calculated with the ZINDO/S

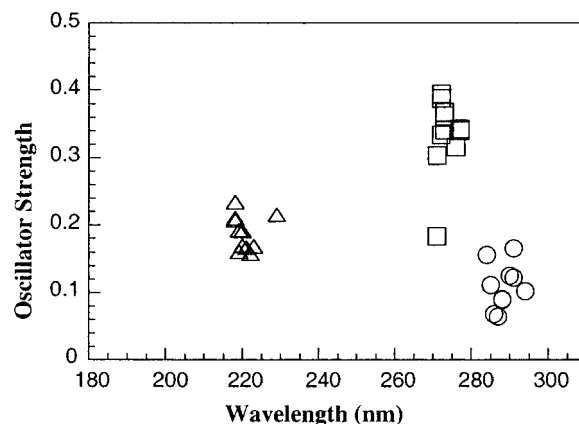


Figure 8. Scatter plot of the three lowest energy transitions and oscillator strength in circles, squares, and triangles, respectively, calculated with the ZINDO/S method for molecules A1, A2, and B with fluorine atoms in different positions.

method using the 201 lowest, singly excited configurations to compute the CI matrix.²³ Shown in Figure 8 with triangles, squares, and circles are the three lowest energy transitions and oscillator strength calculated for isolated molecules having the fluorine atom changed over the four nonequivalent crystallographic positions. The results in Figure 8 suggest that molecular strain and fluorine disorder alone may account for some of the spectral dispersion, but there seems to be no indication of molecular structural factors that may be responsible for the observed red shift.

Intracrystalline Energy Transfer. Dual emission coming from different conformers or different environments in pure and mixed crystalline solids is not rare.²⁴ Selective excitation of surface sites with wavelengths that have low transmission and preferential excitation of bulk molecules with wavelengths that are near the red-edge of the absorption spectrum can also lead to different spectra from the surface and from the bulk.^{18a,b} Dual emission from bulk sites requires incomplete energy transfer and equilibration. For that reason, it is more likely to occur with short-lived species with high radiative rates and/or low rates of energy transfer. As expected for

(23) Hypercube, Inc., Gainesville, FL.

(21) (a) Wang, S.; Bazan, G. C.; Tretiak, S.; Mukamel, S. *J. Am. Chem. Soc.* **2000**, *122*, 1289–1297.

(22) (a) Yamasaki, N.; Inoue, Y.; Yokoyama, T.; Tai, A.; Ishida, A.; Takamuku, S. *J. Am. Chem. Soc.* **1991**, *113*, 1933–1941. (b) Masahide, Y.; Goro, K.; Takumi, N.; Kensuke, S.; Yoshihisa, I.; Noritsugu, Y.; Akira, T. *Bull. Chem. Soc. Jpn.* **1994**, *67*, 505–510.

(24) (a) Lécuyer, R.; Berrehar, J.; Lapersonne-Meyer, C.; Schott, M. *Phys. Rev. Lett.* **1998**, *80*, 4068–4071. (b) Brejc, K.; Sixma, T. K.; Kitts, P. A.; Kain, S. R.; Tsien, R. Y.; Ormo, M.; Remington, S. J. *Proc. Natl. Acad. Sci. U.S.A.* **1997**, *94*, 2306–2311. (c) Vanden Bout, D. A.; Kerimo, J.; Higgins, D. A.; Barbara, P. F. C. D. *J. Phys. Chem.* **1996**, *100*, 11843–11849. (d) Yasuda, M.; Kuwamura, G.; Nakazono, T.; Shima, K.; Inoue, Y.; Yamasaki, N.; Tai, A. *Bull. Chem. Soc. Jpn.* **1994**, *67*, 505–510. (e) Masahide, Y.; Goro, K.; Takumi, N.; Kensuke, S.; Yoshihisa, I.; Noritsugu, Y.; Akira, T. *Bull. Chem. Soc. Jpn.* **1994**, *67*, 505–510.

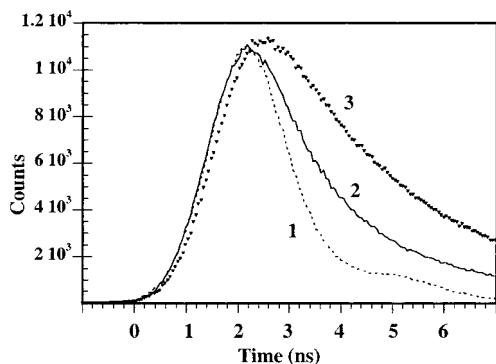


Figure 9. Time dependence of the emission of crystalline **4** under the following conditions: (1) detection of the monomer at 320 nm upon excitation at 300 nm; (2) detection of the aggregate at 430 nm upon direct excitation at 360 nm; (3) detection of the aggregate at 430 nm upon excitation of the monomer.

a sample with absorbers and emitters having different excitation energies and slow equilibration rates, the relative intensities of monomer and excimer emission in the spectrum of **4** (Figure 4) are dependent on the excitation wavelength. We also noticed that fluorescence decay is too complex to be described by simple exponential functions. However, the wavelength dependence of the decay conforms well to the expected energy transfer between species that may undergo exothermic energy transfer. Thus, the time dependence of the aggregate emission detected at 430 nm depends on whether it is excited directly or indirectly by energy transfer from the monomer (Figure 9). Direct excitation of the aggregate at 360 nm gave a time profile with a growth that is parallel to that of the lamp pulse followed by its complex decay (Figure 9, signal 2). In contrast, preferential excitation of the monomer at 300 nm resulted in a ca. 0.3–0.5 delayed growth of the aggregate emission (Figure 9, signal 3). Also shown in Figure 9 is the time dependence of the “quenched” monomer emission excited at 300 nm, which grows with the excitation pulse and decays by fast emission and by energy transfer to the aggregate. Although the lifetimes of the aggregate and monomer emission were too complex to be fitted by two or three exponentials, their decays are consistent with the postulated energy transfer processes.

Phosphorescence Emission and Triplet Yield. Measurements carried out at 77 K in dilute methylcyclohexane glasses revealed a remarkably intense, long-lived, and highly structured phosphorescence between 450 and 600 nm (Figure 10). Phosphorescence decays were fit to a single-exponential function over most of their decays to give lifetimes of 1.4 and 1.0 s for **4** (Figure 10, inset) and **5**, respectively. Measurements carried out at high concentration, under conditions where only aggregate fluorescence was observed, yielded no phosphorescence signal. Phosphorescence emission in the crystalline solid was significantly weaker, less resolved, and red-shifted by about 25 nm with respect to the one observed in solution.¹⁷ The triplet state properties of **4** and **5** are similar to those reported for dilute solutions of diphenylacetylene (tolan) in terms of triplet energies and S_1-T_1 energy gap. The onset of the phosphorescence emission of compounds **4** and **5** corresponds to triplet energies of 63.5 kcal/mol, as compared to 63.4 kcal/mol that was reported previously for tolan.²⁵ A S_1-T_1 energy

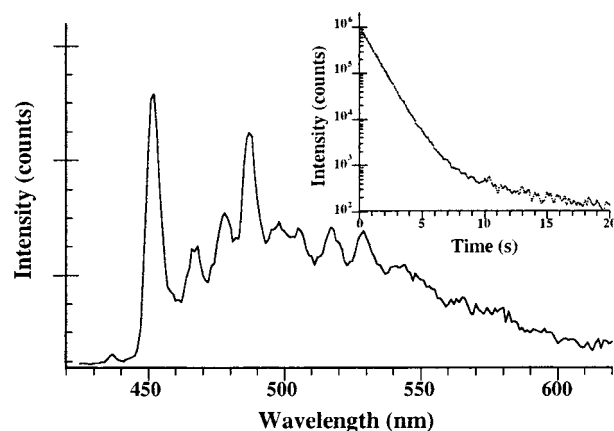


Figure 10. Phosphorescence spectrum of **4** in methylcyclohexane at 77 K and phosphorescence decay in a 20 s window (inset)

gap of 35 kcal/mol calculated from spectra for **4** and **5** compares well with a gap of 32.4 kcal/mol reported for diphenylacetylene. The most significant difference between compound **4**, tolan, and other phenylacetylenes came from the high triplet yields of the former. Whereas tolan has a triplet yield of only $\Phi_T = 0.03$, we determined a lower limit of $\Phi_T = 0.64$ for compound **4** in solution at ambient temperature. The lower limit for the triplet yield of **4** was estimated by measuring the photosensitized generation of singlet oxygen²⁶ with concentrations that were low enough to ensure that only the triplet state could act as a sensitizer. The high triplet yield and intense emission of compound **4** are significantly higher than those of other arylacetylenes.²⁷ This property seems to originate from the presence of the fluorine substituent. It is known that a single fluorine increases the triplet yield of benzene from $\Phi_T = 0.25$ up to $\Phi_T = 0.8$ in fluorobenzene.²⁸ It may be noted that the high triplet yields and relatively strong triplet emission for compounds **4** and **5** bode well for electroluminescence and magneto-optic applications of fluoro-substituted aryl-ethynes and poly(phenylene-ethynylenes).

Conclusions

In this paper, we have analyzed the solution and solid state photophysics of 1,4-diethynyl-2-fluorobenzene **5** and 1,4-bis(2-hydroxy-2-methyl-3-butynyl)-2-fluorobenzene **4**. The singlet state of compound **4** in dilute solution was characterized by a relatively strong fluorescence emission with a $\lambda_{max} = 312$, a quantum yield of $\Phi_F = 0.15$, a lifetime of $\tau_F = 2.0$ ns, and a remarkably high intersystem crossing quantum yield of $\Phi_{ISC} > 0.64$. Dilute samples in methylcyclohexane at 77 K gave excitation and emission spectra that were similar to those observed at ambient temperatures and a fluorescence lifetime of 3.1 ns. Concentrated solutions in the same solvent at 77 K gave rise to aggregate emission with a $\lambda_{max} = 340$ and a lifetime of 8.8 ns. Consistent with relatively high triplet

(25) (a) Evans, D. F. *J. Chem. Soc.* **1957**, 1351–1357. (b) Beer, M. *J. Chem. Phys.* **1956**, *25*, 745–750.

(26) Foote, C. S.; Clennan, E. L. In *Active Oxygen in Chemistry*; Foote, C. S., Valentine, J. S., Greenberg, A., Liebman, J. F., Eds.; Blackie Academic and Professional: New York, 1995.

(27) (a) Walters, K. A.; Ley, K. D.; Schanze, K. S. *Chem. Commun.* **1998**, 115–116.

(28) Sandros, K. *Acta Chem. Scand.* **1969**, *23*, 2815–2829.

yields estimated by singlet oxygen sensitization was a strong, well resolved, and long-lived phosphorescence which was observed only for the monomer in dilute methylcyclohexane solutions cooled to 77 K. The photophysics of concentrated solutions at low temperatures were qualitatively consistent with results obtained in the solid state. Using diffuse reflectance and fluorescence measurements in the solid state, we documented the effects of aggregation on the photophysics of 1,4-diethynylbenzene chromophore for the first time. Spectral bands associated with aggregates were characterized by red shifts of 60–80 nm and by the loss of vibrational structure in both absorption and emission. Along with aggregate emission, a weak fluorescence band assigned to the monomer was also observed in the solid state. Single-crystal X-ray analysis revealed a remarkably rich packing structure with four distinct molecules per asymmetric unit with the fluorine substituent disordered over all the crystallographically nonequivalent aromatic positions. The positional disorder is manifested in terms of multiple overlapping signals in the solid state CPMAS ^{13}C NMR spectra. Among the packing interactions that may be responsible for the aggregate emission, close cofacial contacts were observed in discrete dimeric and trimeric units. We speculated that monomer emission may originate from molecules with no close cofacial

contacts. We were able to document intracrystalline singlet energy transfer from the excited state monomers to the lower excited energy aggregates. We hope that results reported here will prove useful in distinguishing the nature and magnitudes of aggregation and planarization on the photophysics of compounds with alkyne-conjugated aromatic luminophores. Work in progress with 1,4-bis(arylethynyl)arenes and oligo(phenyleneethylenes) is consistent with results presented here.

Acknowledgment. This work was supported by the NSF (Grants DMR9988439 and CHE0073431). Solid state NMR spectra were acquired with equipment purchased with NSF Grant DMR9975975. We thank Prof. Uwe Bunz from the University of South Carolina and Prof. Chris Foote from UCLA for advice. One of us (G.Z.) would like to thank COFAA-IPN (Crédito Educativo No.9911220454), CONACyT (Ref. 990205), and the US-Mexico Commission for Educational and Cultural Exchange (Fulbright-García Robles fellowship).

Supporting Information Available: Phosphorescence spectra, phosphorescence decay, stereoscopic views, and X-ray tables of **3**. This material is available free of charge via the Internet at <http://pubs.acs.org>.

JO015589E